Heat and Mass Transfer (2019) 55:2949–2958
https://doi.org/10.1007/s00231-019-02593-2

ORIGINAL

Experimental and numerical analysis of composite latent heat storage in cooling systems for power electronics

Thomas Bezerra Helbing[1,2] · **Gerhard Schmitz**[1]

Received: 14 December 2018 / Accepted: 7 February 2019 / Published online: 10 May 2019

Abstract

This article presents a validated numerical model of composite latent heat storage (CLHS) used for designing cooling systems for power electronics (PE). Successfully implementing CLHS depends on many factors. Testing all of them on a test rig is expensive and time consuming. A CLHS model allows system designers to test CLHS in complex applications by varying dimensions and operating conditions. The model is written in the equation-based modelling language Modelica and represents the melting process of three-dimensional discretised CLHS. In order to validate the model a test rig is built and validation results are shown. The validated CLHS model is used in two different cooling systems. The first system is an air cooling system for power electronics with a high dynamic behaviour and lower power output. The second cooling system is a more complex liquid cooling system with a significantly increased power output. The article shows and discusses the results of both system simulations.

Nomenclature

ρ	density	(kg/m^3)
B	liquid fraction	(-)
C	heat capacity	(J/K)
c	specific heat capacity	(J/kg K)
c_0	specific heat capacity of solid material	(J/kg K)
c_b	constant	(-)
h_f	latent heat	(J/kg)
k	thermal conductivity	(W/(m K))
$\dot{m}$	mass flow rate	(kg/s)
$\dot{Q}$	heat flow rate	(W)
R_th	heat resistance	(K/W)
T	temperature	(°C)
T_f	melting temperature	(°C)
t	time	(s)
x	dimensional Cartesian coordinate	(m)

AC	Alternating Current
CAD	Computer-Aided Design
CLHS	Composite Latent Heat Storage
CP	Cold Plate
DC	Direct Current
DSC	Differential Scanning Calorimetry
FEM	Finite Element Method
LHS	Latent Heat Storage
PCM	Phase Change Material
PE	Power Electronics
PGW	Propylene Glycol Water
SHS	Sensible Heat Storage
TIM	Thermal Interface Material

1 Introduction

Due to increasing demand in converting and controlling electric power, e.g. electrification of vehicles and increasing installation of wind or solar power plants, the use of power electronics has steadily increased over the last years. Despite improved efficiency of semiconductors, miniaturization of electronic modules still leads to high heat loss densities. Therefore, efficient and well-designed cooling systems are required to avoid failures due to high temperatures. In many cases, space and/or weight is limited.

✉ Gerhard Schmitz
schmitz@tuhh.de

Thomas Bezerra Helbing
thomas.helbing@jungheinrich.de

[1] Institute of Engineering Thermodynamics, Hamburg University of Technology, Denickestr. 17, 21073 Hamburg, Germany

[2] Present address: Jungheinrich Norderstedt AG & Co. KG, Lawaetzstr. 9-13, 22844 Norderstedt, Germany

Power electronics are used in a wide field of applications. Designing a cooling system depends on the operating conditions. One way of classifying these operating conditions is to divide them into systems with constant power output and systems with variable power output.

Cooling systems of applications with constant power output most of the time operate in steady state with a developed temperature field. In this case, the focus in designing the cooling system is on reducing the heat resistance to ambient. The heat capacity of the cooling system is mainly required for the starting process. In most cases, the cooling system can be dimensioned according to the heat flow rate of the steady state operating point.

Dynamic electric systems with variable power output often do not reach a steady state. Depending on its dynamic behaviour, a cooling system has to be dimensioned according to the maximum heat loss to avoid overheating. Such a system is oversized at all other operating points. A common solution for increasing the heat capacity of the cooling system is to use more material, e.g. copper or aluminium. In this case, higher heat resistance and mass of the material have to be taken into account. A heat storage using the heat capacity of a material is called sensible heat storage (SHS).

An alternative to a SHS is a latent heat storage (LHS). Latent heat is thermal energy absorbed or released during the phase change of a material. Materials changing phases are called phase change materials (PCMs). Commonly used PCMs are paraffins and salt hydrates. They can store large amounts of thermal energy during a phase change while maintaining an almost constant temperature. The main disadvantage of PCMs is their very low thermal conductivity which causes insufficient heat distribution. Heat distribution can be improved by using frame structure of a material with high thermal conductivity. LHS with a frame structure is called composite latent heat storage (CLHS).

Several studies on LHS for cooling electronic devices have been conducted in the last decades. Most of the studies focus on improving the frame structure of CLHS or the material properties themselves.

Ashraf et al. [1] perform experimental analysis of circular and square pin-fins with staggered and inline arrangements. Best cooling performance is achieved by staggered arrangement and circular pin-fins. The influence of the fin length and width on cooling performance has been carried out by Bondareva and Sheremet [3]. The melting time is almost identical when the fin width is decreased while keeping the storage volume constant. Increasing the fin elongation leads to a significantly reduced melting time and in consequence a better cooling performance. Lohse and Schmitz [8] present assessment parameters for CLHS based on simulations using the finite element method (FEM). The assessment parameters are helpful for the evaluation of CLHS. Sahoo et al. [11] give an overview of thermal conductivity enhancers. Thermal conductivity cannot only be enhanced by using specific aluminium structures, but also by using unstructured metallic foams or additives like nano particles. They also point out the importance of the solidification time for cyclic operation.

In Bondareva and Sheremet [2] natural convection of PCM in a square cavity has been investigated numerically. The influence of Rayleigh number, Stefan number and Ostrogradsky number on the melting process is carried out.

Veelken and Schmitz [13] mathematically optimize fins for hot-spot cooling. Results have shown that optimized fin geometry reduces hot-spot temperature up to 2 K. Pizzolato et al. [10] introduce a design approach for a topology optimization of fins in a shell and tube latent heat storage. They focused on reducing the melting and solidification time. Frame structures optimized for melting are different from those optimized for solidification. The melting time with optimized structure can be reduced by up to 37%.

Some studies are more focussed on applications. Ianniciello et al. [4] show how CLHS are implemented into passive and semi-passive cooling systems for lithium ion battery cooling. Several ways of enhancing the performance of a PCM in thermal management are pointed out. Ling et al. [6] present a review on PCM used for thermal management of electronic components. Kinkelin et al. [5] focus on analysing theoretically and experimentally PCMs as thermal damper for cooling electronic devices. A cycle test with up to 1000 cycles proves a high stability of PCM regarding latent heat.

This study put the focus on the system level and its main objective is to show how implementing CLHS in a cooling system can improve the cooling performance. Another objective is to point out the benefits of a system simulation for an application-orientated assessment of CLHS.

Therefore, a numerical model of CLHS is created and validated using experimental data. This model is used in a system simulation representing typical applications with highly variable power output, e.g. lifting materials. This study shows several system simulations and analyses their results.

2 Numerical model

A CLHS model has to describe two physical processes: thermal conductivity and the phase change process. Simulating the latter is more challenging.

Since the phase change process depends on the temperature field of material, a fine discretisation of the model is

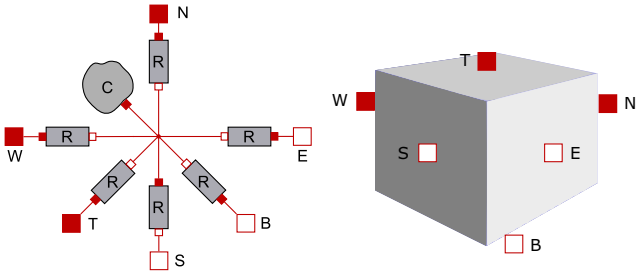

Fig. 1 Structure of a thermal conductance model in Modelica

required. Modern FEM tools are capable of simulating very finely discretised CLHS models with low computation time. This is the reason why in most studies FEM tools are used for the numerical analysis of a single component or less complex systems.

As far as larger systems are concerned, FEM tools are not adequate anymore and system simulation tools are necessary. System simulation models are often less detailed, e.g. map-based models. However, a CLHS requires a physical model with a higher level of detail.

One way of combining both approaches is to perform a co-simulation. This kind of simulation is non-trivial and can lead to numerical difficulties. A more productive way is to use a single tool. As it is more convenient to create a locally discretised model with a system simulation tool than to create a system model with a FEM tool, the CLHS model is created with a system simulation tool based on the modelling language Modelica.

2.1 Model description

Modelica is an acausal, object-oriented and multi-domain modelling language that provides libraries with e.g. electric, hydraulic, and thermal system components. The design of the CLHS model is described in the following.

One way of modelling CLHS in Modelica is to use hierarchical models. These are based on basic models which are instantiated with values and connected to each other. Figure 1 shows a basic model of a solid block representing the thermal conductivity and heat capacity of a body.

The solid block is based on transient, 1-dimensional heat conduction equation derived from first law of thermodynamics and Fourier's law:

$$\rho c \frac{\partial T}{\partial t} = k \frac{\partial^2 T}{\partial x^2}. \tag{1}$$

The model of the solid block is divided into two sub models, the heat resistor (R) and the heat capacitor (C). These sub models are designed in analogy to electrical components.

The heat resistor is only valid for one axial direction (one-dimensional). It represents the stationary part of the model $\left(\frac{\partial T}{\partial t} = 0\right)$

$$\frac{\partial^2 T}{\partial x^2} = 0 \tag{2}$$

which is described for flat walls in analogy to Ohm's law as:

$$R_{th} = \frac{T_2 - T_1}{\dot{Q}}. \tag{3}$$

The transient part of the heat conduction equation is described in the heat capacitor model by:

$$\frac{\mathrm{d}T}{\mathrm{d}t} = \frac{\dot{Q}}{\rho V c} = \frac{\dot{Q}}{C}. \tag{4}$$

As the heat resistor is one-dimensional at least three heat resistors are required to represent all axial directions. In order to position the heat capacity in the centre of the block the number of heat resistors is doubled and the heat resistance value in each direction is halved. The six heat resistors are connected to the heat capacitor. Heat transfer into and out of the solid block are realized by the heat connectors N,S,W,E,T, and B, two for each spatial direction.

The model shown in Fig. 1 describes a solid block without phase change. The PCM model is basically the same model, but uses a different heat capacitor model. Instead of a fixed heat capacity, the model uses a temperature-dependent heat capacity which significantly increases during the phase change of the material. This approach is called effective heat capacity method. Equations and the approach are described in [7].

The following exponential function for a smoothed step has been implemented:

$$c_{\mathrm{PCM}} = c_0 + \Delta h_{\mathrm{f}} \frac{c_{\mathrm{b}} e^{-c_{\mathrm{b}}(T - T_{\mathrm{f}})}}{(1 + e^{-c_{\mathrm{b}}(T - T_{\mathrm{f}})})^2}. \tag{5}$$

c_0 is the heat capacity of the solid material, Δh_{f} the latent heat, T_{f} the melting temperature and c_{b} a parameter for the melting temperature range. The value of c_{b} is defined by adjusting the exponential function to the data of the PCM's differential scanning calorimetry (DSC). Volume increase during phase change is neglected.

In theory, a solid block model represents small solids as well as large solids. However, a solid block model cannot describe a temperature field. It features only one temperature value in the centre and six temperature values on the outside. In order to describe a temperature field, it is necessary to discretise the solid blocks by instantiating the model depending on the discretization parameters and to connect the discrete elements with each other. The connection is done by for-loops.

Experience has shown that this kind of modelling is time-consuming with regard to the computation time.

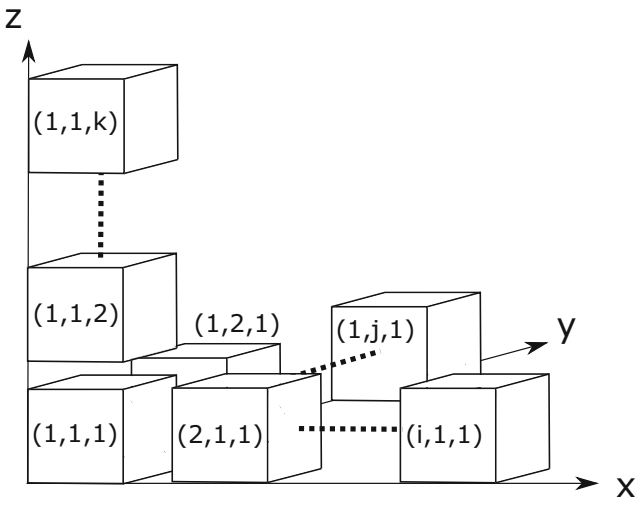

Fig. 2 Schematic diagram of the matrix-based discretisation and the indices i, j and k

An alternative to the hierarchical modelling is matrix-based modelling. Instead of instantiated models, the main model uses several three-dimensional matrices. Geometry parameters, material properties and temperature values of CLHS are represented by one matrix each. Matrix indices define the position of the discrete elements. Matrix entries represent the parameters of the discrete elements.

A matrix is used to distinguish between aluminium and PCM. The matrix has two types of entries, 0 is aluminium and 1 is PCM. Depending on this matrix entry material properties and calculations are defined for each discrete element.

Interaction between the discrete elements and the phase change process is realized by simple matrix calculations. The equations are the same as in the hierarchical model. The phase change is described by a three-dimensional matrix with the following entries:

$$c_{\mathrm{PCM,ijk}} = c_0 + \Delta h_{\mathrm{f}} \frac{c_{\mathrm{b}} e^{-c_{\mathrm{b}}(T_{\mathrm{ijk}} - T_{\mathrm{f}})}}{(1 + e^{-c_{\mathrm{b}}(T_{\mathrm{ijk}} - T_{\mathrm{f}})})^2}. \tag{6}$$

The indices i, j and k describe coordinates of the discrete elements. A schematic diagram of the matrix-based discretisation is shown in Fig. 2.

This approach improves the computation time and increases the possibility of integrating a CLHS model into a complex system. Since the geometry is defined by a matrix, new structures can be integrated using a matrix made of computer-aided design (CAD) data.

Table 1 shows CLHS materials and their properties. All simulations and experiments use the paraffin *PARAFOL 22-95®* as a PCM. *PARAFOL 22-95®* has a melting temperature of 41.6 °C and a latent heat of 250 kJ/kg. The CLHS' frame structure is made of aluminium *ENAW 2007* aluminium.

Table 1 Material properties of ENAW 2007 and *PARAFOL 22-95®* [12]

Property	*ENAW 2007*	*PARAFOL 22-95®*
Density ρ in kg/m^3	2850	777
Specific heat capacity c in J/(kg K)	900	3300
Thermal conductivity k in W/(m K)	160	0.162
Melting temperature in °C	–	41.6
Latent heat in kJ/kg	–	250

3 Experimental analysis

In order to validate the model a test rig was built. The test set-up and the validation of the Modelica model using experimental data is described in the following.

3.1 Set-up

The test rig consists of the CLHS and a power electronic dummy. The power electronic dummy is pressed on the CLHS with two polycarbonate plates and four threaded rods. Thermal interface material (TIM) with a thermal conductivity of 10 W/(m K) reduces the contact resistance between the components. Rubber foam pads reduce heat loss to the ambient.

Figure 3 shows an exploded view of the CLHS. Since a complex structure, e.g. metal foam, cannot be represented by the Modelica model, a finned structure is used as a frame structure. Finned structures have already been used successfully as frame structures in the past [7].

When using paraffins as PCMs, the increase in volume during the phase change from solid to liquid is especially challenging. This problem is solved by using a silicone membrane which allows the paraffin to expand into a chamber. When the PCM solidifies, the membrane presses the PCM back between the fins. Furthermore, the membrane seals the rear of the CLHS. The sight glass on the front allows to observe the phase change process with a monochrome camera.

The total mass of the CLHS with sight glass, expansion chamber and screws is 383 g. The aluminium frame structure has a mass of 168 g and the mass of PCM is 44 g. The CLHS has a PCM volume fraction of 51.4%. In real applications the volume fraction can be increased for improved performance by leaving the aluminium flanges out.

The power electronic dummy is an aluminium block with two heating cartridges inside. A DC power supply with an accuracy of $\pm(0.2\% + 3$ digits) regarding voltage and current controls the electric power of the cartridges. By

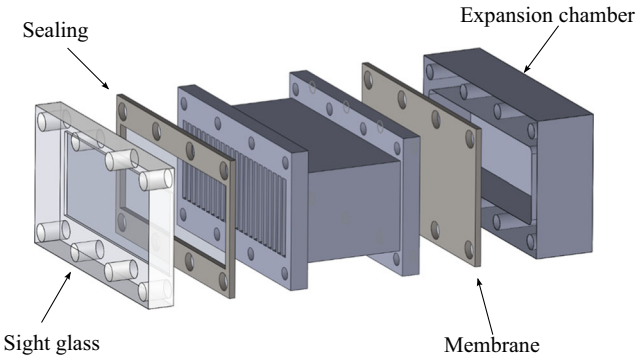

Fig. 3 Exploded view of the CLHS

using Ohm's law current and voltage are adjusted. Dynamic heat load profiles are possible.

The junction temperature of the power electronic dummy is measured by five thermocouples soldered directly under the contact surface of the power electronic dummy. The PCM temperature is measured by three thermocouples placed at different levels inside the PCM container. Figure 4 shows the position of these thermocouples and the position of the power electronic dummy.

The test is monitored by a *National Instruments data acquisition* system with *LabVIEW 2013*. All thermocouples (type T) are calibrated for a temperature range of 0–100 °C. The maximum variation is ±0.15 °C.

The set-up has been mounted and dismounted four times and tested with the same heat load profile. Each time TIM is renewed. The repeating accuracy of this set-up is ±1 °C.

3.2 Model validation

The test set-up is mapped in Modelica. The CLHS geometry is described by a matrix generated out of CAD data. A block model of aluminium represents the power electronic dummy. To represent the heat capacity of additional components, models of the sight glass, the expansion chamber and the polycarbonate plates are implemented as discretised solid blocks. All models are connected to each other and parameterised. During the test, a heat load profile is recorded and defined as an input to the simulation.

The validation is performed by a heating-up scenario. From the beginning, the heat cartridges deliver an 80 W heat flow rate. After 440 s the power is turned off. Test and simulation start at 20 °C.

Figure 5 shows the melting process in the simulation and in the experiment at different points in time. The pictures of the monochrome camera are reworked to visualise the melting front of the PCM, thus allowing for a better comparison with the simulation. In the simulation the liquid fraction of the PCM blocks near the sight glass is

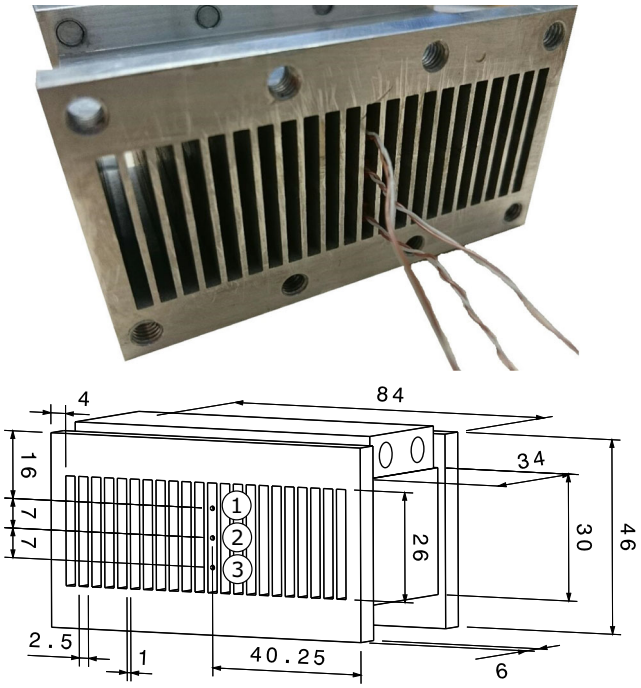

Fig. 4 Measuring positions and dimensions (in mm) of the CLHS with heating block mounted on the top

used. The white areas are liquid PCM and the black solid PCM.

The melting front of the simulation and the melting front of the experiment match well. The slower melting process in the experiment is due to heat loss to the ambient, which

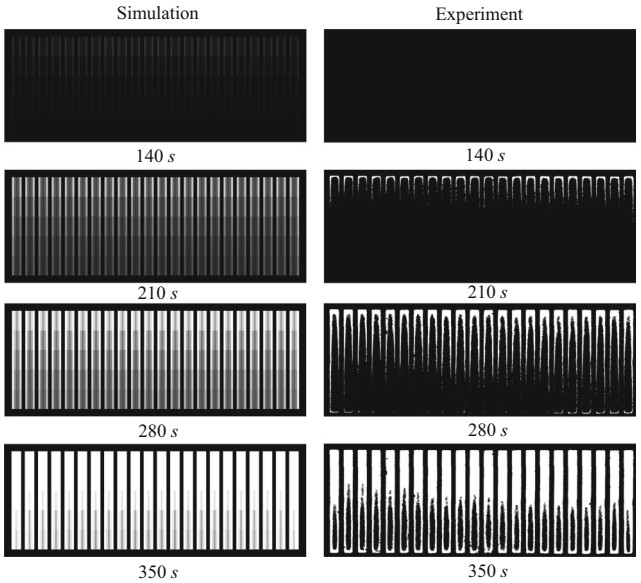

Fig. 5 Comparison of the melting process in the simulation and in the experiment. White is liquid and black is solid

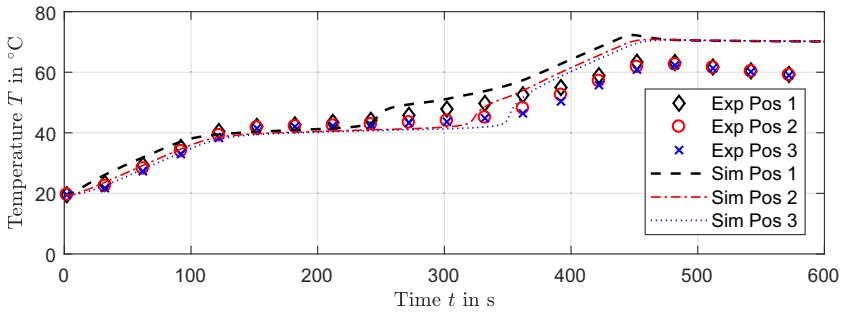

Fig. 6 Comparison of the PCM temperature in the simulation and in the experiment

is hardly to prevent. Nevertheless, the simulation represents the local melting process very well.

Figure 6 shows the PCM temperature results. Due to the complex melting process of the PCM and its thermal inertia, the three measuring points inside the PCM are used for validation. Temperature differences between simulation and experiment are more distinctive in PCM than in aluminium.

At the beginning, the temperature rises nearly linearly. The temperature difference between the positions in the simulation is higher than in the experiment. The temperature at the measuring point near the power electronic dummy is higher. After 110 s, the temperature stops rising at about 40 °C and forms a temperature plateau. Up to 250 s the simulation matches the experimental results very well. As soon as the PCM has liquefied, the temperature rises again. The higher the temperature the higher is the mismatch between simulation and experiment. Just before turning off power, the temperature difference between the averaged simulation temperature and the averaged experiment temperature is 8.5 °C.

By turning off power at 440 s the CLHS strive to achieve thermal equilibrium and in consequence the temperature at the three measuring positions approaches each other. At the end of the simulation the temperature is almost steady state. In contrast, the temperature of the experiment drops to nearly 60 °C which is caused by heat loss to ambient. Even with heat insulation temperature drop cannot be avoided completely. It is assumed that the copper cables of the heat cartridges are one of the main causes of heat loss. All in all, the model shows good results.

4 System simulation

The validation has proven that the system model represents a CLHS very well. Systems with dynamic heat load profiles benefit a lot from the use of CLHS. One possible application for a CLHS is a PE of an electrical construction machine or industrial truck. PE is needed to transform the current from direct current (DC) to alternating current (AC), if the electric motor obtains the electric energy from a battery. These machines have usually electric motors for the movement of the vehicle and electric motors for lifting. In many cases the motor for lifting is larger than the motor for movement. A discontinuous use of the lifting motor leads to an extremely dynamic heat flow rate.

This application is the basis for the following system simulations. Alternative applications are electric motors with discontinuous behaviour in aviation or automotive.

As an example two scenarios are shown. The first scenario represents an air-cooled PE with lower power output. The second scenario has a significant increased power output which is cooled by a liquid cooling system. The simulation set-up and the results of both scenarios are shown in the following.

4.1 Air cooling system

The CLHS model is adapted to a larger and flatter geometry than in the validation. The geometry and the dimensions are shown in Fig. 7. This CLHS has a volume fraction of 54.9%.

Natural convection on the outer surface is represented by a model of the *Modelica Standard Library* [9]. The heat transfer coefficient is set to a value of 50 W/(m^2 K), which is 5–10 times higher than for natural convection and describes an active cooling by a fan. For a detailed analysis of the electronics, models of electronic libraries can be used to simulate the electric circuit. As the focus in this study is on thermal behaviour of CLHS the PE is represented by a simple heat source model which transfers an user-defined heat flow rate.

In order to represent a design scenario with the worst case boundary conditions the ambient temperature and the starting temperature are set to 40 °C. The melting

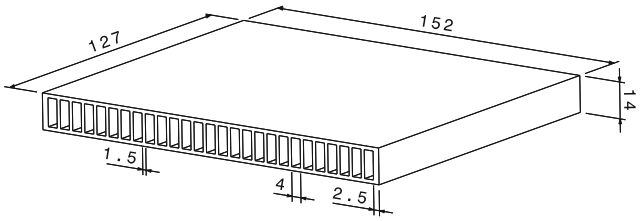

Fig. 7 Scenario I: Drawing of the CLHS (in mm)

temperature of the PCM is set to 60 °C. Other material properties are identical to Table 1.

Figure 8 shows the heat load of the PE. Starting at 200 s every 60 s the system is heated up by a rectangular peak with a maximum value of 300 W. Each peak has a duration of 10 s and represents one process step (e.g. lifting material to maximum height).

Two simulations are carried out. The first simulation uses a CLHS. In the second simulation the CLHS is replaced by a SHS with the same mass as CLHS.

Figure 9 shows the temperature on the heat source of both simulations. Each peak in the heat flow rate leads to a peak in the temperature. Afterwards the temperature is reduced by heat distribution in the CLHS and heat transfer to ambient. The average temperature of the SHS is asymptotically tending to almost 83 °C. At the beginning, the temperature behaviour of CLHS is comparable to SHS. When the junction temperature reaches 60 °C a temperature plateau is obtained for several peaks. After 1400 s, power is turned off.

The liquid fraction of the PCM is shown in Fig. 10. Each peak leads to an increase of the liquid fraction. After each peak, the liquid fraction drops slightly, but the regeneration time is too short for a significant solidification of the PCM. At the end of the heating-up, all PCM is liquid.

This scenario shows the importance of the correct sizing of the CLHS. Since all PCM is liquid after the last peak, a longer heating time would lead to a significant temperature increase. The benefit towards the SHS is lost when the CLHS is operated with completely liquid PCM.

The simulation shows also the high regeneration time of a CLHS. The stored thermal energy has to be released over a longer period of time than with the SHS.

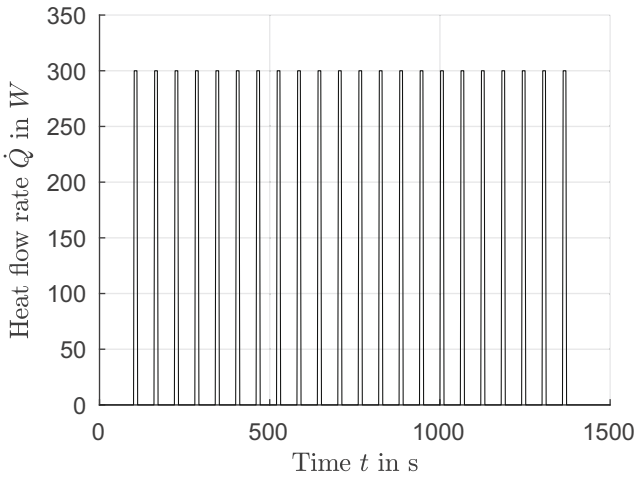

Fig. 8 Scenario I: heat flow rate of PE

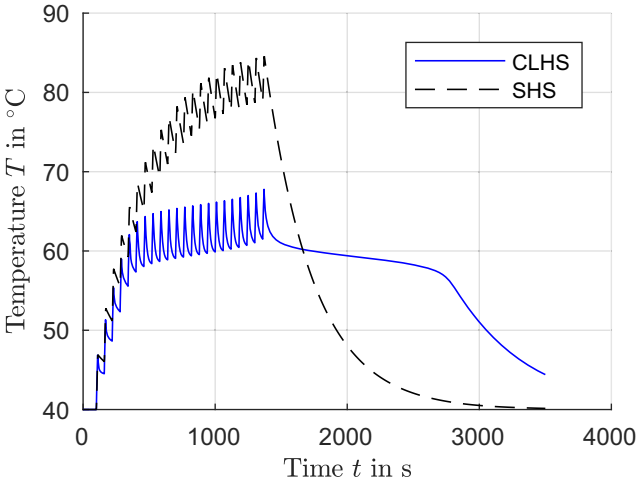

Fig. 9 Scenario I: maximum temperature of the simulation with CLHS and SHS

4.2 Liquid cooling system

In the second scenario, a CLHS is used in a liquid cooling system. Figure 11 shows a schematic diagram of this cooling system, which is rebuilt and parametrised in Modelica.

A pump transports the fluid, a 60/40 propylene glycol water (PGW) mixture, through an air-liquid heat exchanger. In the heat exchanger PGW is cooled down by ambient air with a temperature of 40 °C. The liquid enters a tubed cold plate (CP) and is heated up.

Three simulations with different assemblies are carried out. The first simulation uses a four-way tubed cold plate with an integrated CLHS. The drawing of the cold plate is shown in Fig. 12. The dimensions of PCM chambers are unchanged from scenario I (Fig. 7). In the second

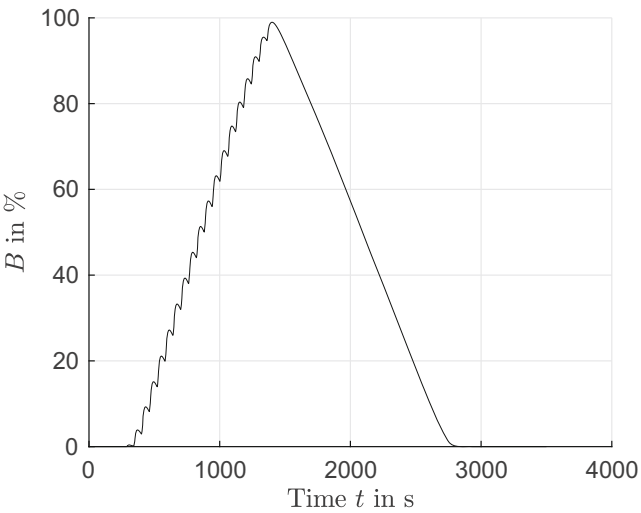

Fig. 10 Scenario I: liquid fraction of the PCM

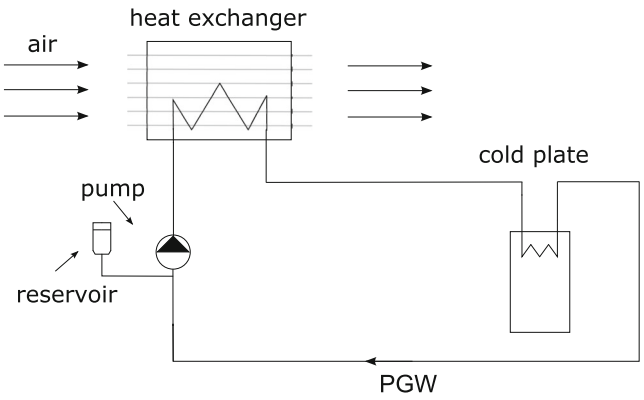

Fig. 11 Schematic diagram of the liquid cooling system

simulation, the CLHS is replaced by a SHS with the same mass as that of the CLHS (472 g). The height is reduced from 26.7 mm to 21.3 mm while width and length are kept constant. In the third simulation a reference system without any heat storage is used. The height of the component is reduced to 12.7 mm. The tube dimensions of the cold plate are identical for all simulations. The melting temperature of the PCM is set to 60 °C.

Two PE are mounted on each assembly. A PE (PE1) with a constant power output of 200 W is mounted on the top side. In this position the heat resistance to the cooling fluid is lower, which ensures a smaller temperature gradient in steady state.

The second PE (PE2) is mounted on the opposite side. This PE has a discontinuous power out. As CLHS and SHS are positioned between PE and CP they buffer the thermal impact and reduce the temperature during the peak. After the peak the heat is transferred through the fluid to ambient.

The heat flow rate of the second PE is shown in Fig. 13. Five peaks with a maximum heat flow rate of 1500 W and a duration of 40 s transfer a high amount of thermal energy into the cooling system. The first peak starts at 300 s and the other follow every 300 s.

Figure 14 shows the heat source temperature results. All simulations start with a heat source temperature of 40 °C. At the beginning, the temperature of all simulations rises due to the constant heat flow rate of PE1. The temperatures approach a steady state temperature of nearly 52.6 °C. After

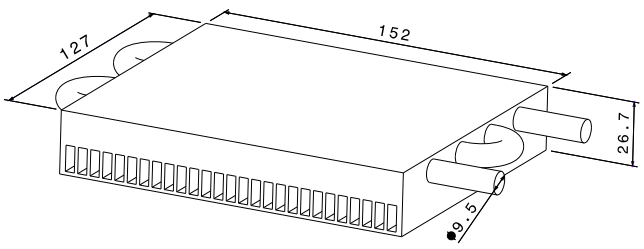

Fig. 12 Scenario II: drawing of the CLHS with cold plate (in mm)

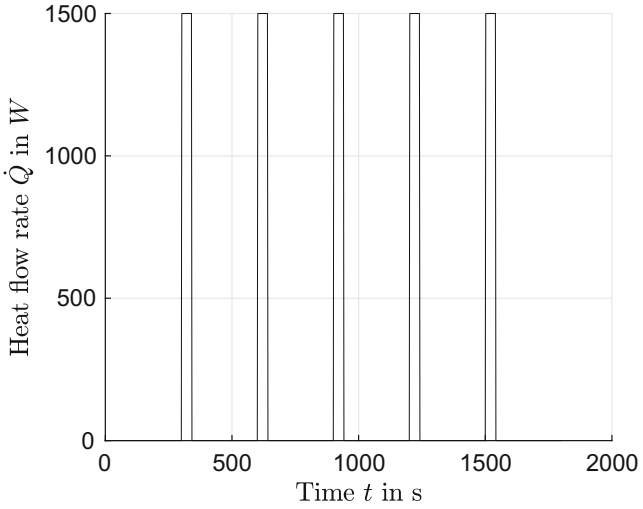

Fig. 13 Scenario II: heat flow rate of PE with discontinuous power output

300 s the first peak increases the temperature immediately. In the reference system the temperature rises to 119.4 °C. The temperature of the system with SHS rises to 99.1 °C and with the CLHS to 82.4 °C. The CLHS stores a high amount of thermal energy during the peak. On the last peaks the maximum temperature of the reference system and with SHS remains nearly the same. The temperature of the system with CLHS increases to a value of 88.7 °C. This temperature increase is caused by missing solidification time of the PCM between the peaks.

The liquid fraction of the PCM is shown in Fig. 15. Almost 90% of the PCM is liquid after the first peak. Between the first and the second peak, the liquid fraction drops to 40%. The amount of solid PCM is too low for the

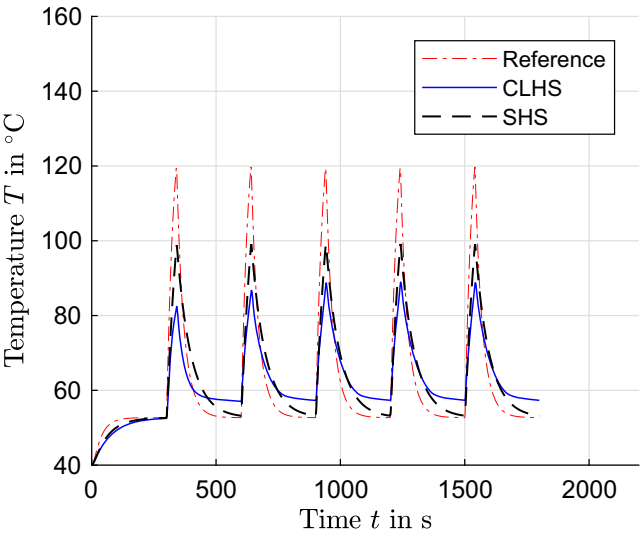

Fig. 14 Scenario II: maximum temperature of PE1 in the reference system, the system with CLHS and SHS

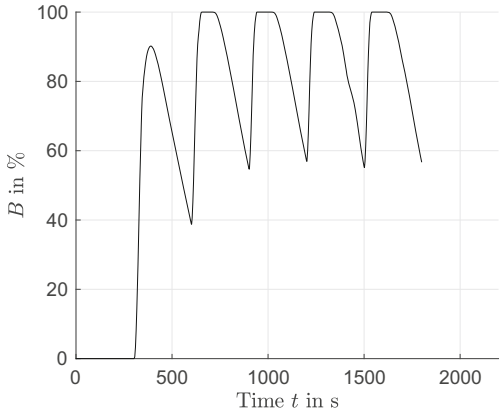

Fig. 15 Scenario II: liquid fraction of the PCM

second peak and in consequence the liquid fraction reaches a value of 100%. The liquid fraction remains for a certain time at this value, which leads to a higher temperature. The thermal behaviour of the following peaks is nearly stationary. The liquid fraction drops slightly to a value below 60% and rises again to 100% for several times.

In this scenario CLHS reduces the temperature significantly. CLHS buffers the peaks and is a light-weight alternative to SHS. As mentioned in scenario I the benefit of CLHS depend on the specific scenario and the correct sizing. CLHS used in temperature regions above the phase change temperature are not effective. The overall temperature rises and the performance of the cooling system decreases. System simulations support the design of cooling systems with CLHS.

5 Conclusions

This article shows an efficient system model for CLHS with finned frame structures designed in the modelling language Modelica. A comparison of junction temperature in simulation and experiment shows a very good agreement. At higher temperatures the gap between experiment and simulation values is slightly increased caused by heat loss to ambient in the experimental set-up. The validated model can be used for system simulation in large and complex systems.

The CLHS model is implemented into two different systems. In the first scenario, an air-cooled PE of a construction machine or industrial truck is represented. Simulations with CLHS and SHS are performed. SHS with same mass as CLHS has an almost 20 °C higher temperature. After the heating period, the solidification of PCM remains the temperature at a high level while the SHS temperature drops continuously. Nevertheless, in cooling systems with dynamic behaviour and sufficient regeneration time a well-sized CLHS is a lightweight alternative to SHS.

The second scenario is an active liquid cooling system for machines with higher power demand. Two PE are mounted on the cooling assembly. One with a constant power output and one with dynamic power output. Simulations are carried out without heat storage, with CLHS and with SHS. Compared to the reference system CLHS reduces the maximum temperature by 30.7 °C. The maximum temperature of CLHS is 10.4 °C lower than in SHS.

Both scenarios show the importance of analysing CLHS at system level in order to evaluate the cooling performance under more realistic conditions.

Compliance with Ethical Standards

Conflict of interest On behalf of all authors, the corresponding author states that there is no conflict of interest.

References

1. Ashraf MJ, Ali HM, Usman H, Arshad A (2017) Experimental passive electronics cooling: parametric investigation of pin-fin geometries and efficient phase change materials. Int J Heat Mass Transf 115:251–263. https://doi.org/10.1016/j.ijheatmasstransfer.2017.07.114
2. Bondareva NS, Sheremet MA (2017) Flow and heat transfer evolution of PCM due to natural convection melting in a square cavity with a local heater. Int J Mech Sci 134:610–619. https://doi.org/10.1016/j.ijmecsci.2017.10.031
3. Bondareva NS, Sheremet MA (2018) Conjugate heat transfer in the PCM-based heat storage system with finned copper profile: application in electronics cooling. Int J Heat Mass Transf 124:1275–1284. https://doi.org/10.1016/j.ijheatmasstransfer.2018.04.040
4. Ianniciello L, Biwolé PH, Achard P (2018) Electric vehicles batteries thermal management systems employing phase change materials. J Power Sources 378:383–403. https://doi.org/10.1016/j.jpowsour.2017.12.071
5. Kinkelin C, Lips S, Soupremanien U, Remondière V, Dijon J, Le Poche H, Ollier E, Zegaoui M, Rolland N, Rolland PA, Lhostis S, Descouts B, Kaplan Y, Lefèvre F (2017) Theoretical and experimental study of a thermal damper based on a CNT/PCM composite structure for transient electronic cooling. Energ Convers Manage 142:257–271. https://doi.org/10.1016/j.enconman.2017.03.034
6. Ling Z, Zhang Z, Shi G, Fang X, Wang L, Gao X, Fang Y, Xu T, Wang S, Liu X (2014) Review on thermal management systems using phase change materials for electronic components, Li-ion batteries and photovoltaic modules. Renew Sust Energ Rev 31:427–438. https://doi.org/10.1016/j.rser.2013.12.017

7. Lohse E (2013) Design of regularly structured composite latent heat storages for thermal management applications: Zugl.: Hamburg-Harburg, Techn. Univ., Diss., 2013, 1st edn. Thermodynamik, Dr. Hut, München
8. Lohse E, Schmitz G (2012) Performance assessment of regularly structured Composite Latent Heat Storages for temporary cooling of electronic components. Int J Refrig 35(4):1145–1155. https://doi.org/10.1016/j.ijrefrig.2011.12.011
9. Modelica Association (2018) http://modelica.org
10. Pizzolato A, Sharma A, Maute K, Sciacovelli A, Verda V (2017) Design of effective fins for fast PCM melting and solidification in shell-and-tube latent heat thermal energy storage through topology optimization. Appl Energy 208:210–227. https://doi.org/10.1016/j.apenergy.2017.10.050
11. Sahoo SK, Das MK, Rath P (2016) Application of TCE-PCM based heat sinks for cooling of electronic components: a review. Renew Sust Energ Rev 59:550–582. https://doi.org/10.1016/j.rser.2015.12.238
12. Sasol North America (2016) Parafol® single cut paraffins – technical bulletin. http://www.sasolnorthamerica.com/products/phase-change-materials
13. Veelken H, Schmitz G (2016) Optimization of a composite latent heat storage (CLHS) with non-uniform heat fluxes using a genetic algorithm. Int J Heat Mass Transf 101:600–607. https://doi.org/10.1016/j.ijheatmasstransfer.2016.04.121